10

Improving Air-Conditioners' Energy Efficiency Using Green Roof Plants

Fulin Wang[1] and Harunori Yoshida[2]
[1]*Tsinghua University, Beijing,*
[2]*Okayama University of Science, Okayama,*
[1]*China*
[2]*Japan*

1. Introduction

Environment and energy issues are considered to be most urgent things nowadays even in future. A lot of researches have been conducted to study how to prevent global warming and reduce energy consumption. In the field of building and urban environment, green roof attracts a lot of researchers' attention because it is considered to be a good solution for improving urban thermal environment by mitigating heat island and to reduce building cooling energy consumption by reducing cooling load. Alexandria et al. (2008) analyzed how much the urban canyon temperature can be decreased due to green walls and green roofs. Takebayashi et al. (2007) compared the building surface heat transfer of green roofs with common roofs and high reflection roofs. Kumar et al. (2005) developed a mathematical model to evaluate the cooling potential and solar shading effect of green roofs. Wong et al. (2003) analyzed the thermal benefits of green roofs in tropical area. Di et al. (1999) measured an actual green wall to analyze how much cooling effect is achieved. Elena (1998) analyzed the cooling potential of green roofs. Besides studying the green roofs' benefits of heat island mitigation and thermal isolation, the cost vs. benefit is also analyzed (Clerk et al., 2008) and green roof plants selection is analyzed as well (Spala et al., 2008).

However, researchers seldom focus on how to improve air-conditioners' energy efficiency utilizing the cooling effect and solar shading of green roof plants. Therefore this chapter describes a new system combining the green roof plants with air-conditioners outdoor units for the purpose of utilizing the cooling effect and solar shading of green roof plants (Wang et al, 2008, 2009). Figure 1 shows the structure of the combination system. The outdoor units of air conditioner are set under the plants and let air flow through plants and cooled down by plants. Also the plants shade solar radiation to prevent the outdoor unit from absorbing solar energy and raising surface temperature.

2. System design

Different type of green roof plants, including tree, grass, moss, vine, etc. can be used to construct the system. Different type of plant needs different system structure.

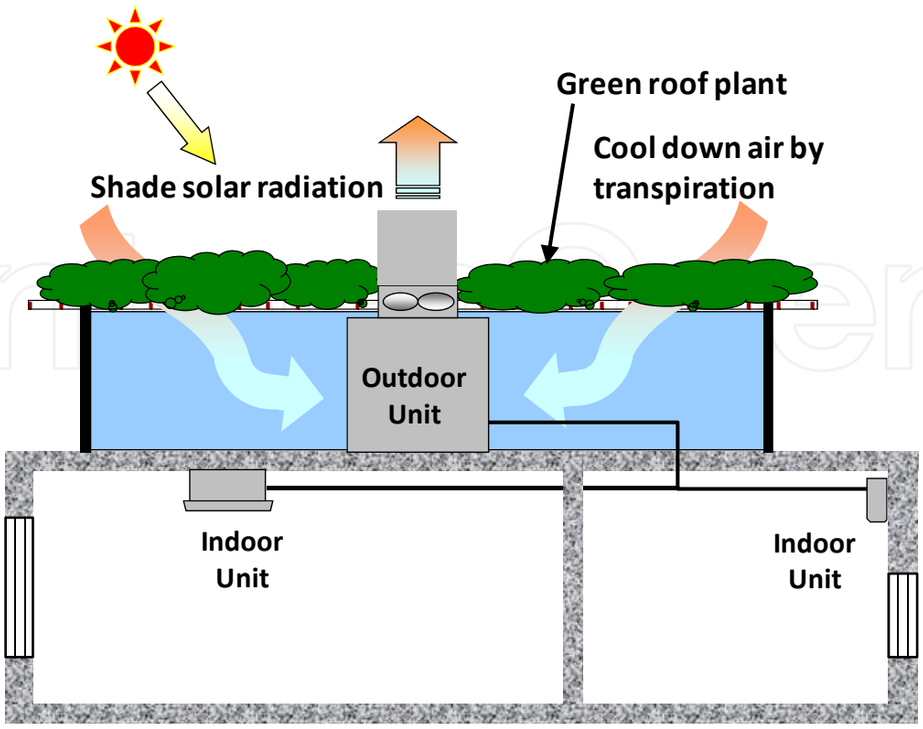

Fig. 1. The system combining the green roof plants with air-conditioner outdoor units.

2.1 Trees

Outdoor units of air-conditioner can be put under threes (Figure 2). Trees can shade solar radiation to prevent outdoor unit from absorbing solar radiation. Trees can cool down air as well by transpiration and the cooled air flows down and is sucked into air-conditioner outdoor units.

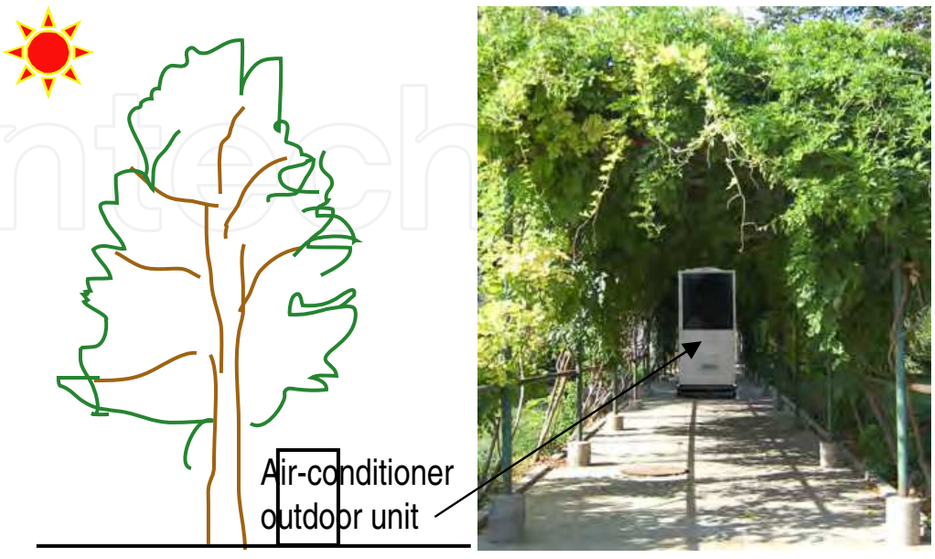

Fig. 2. Combination of air-conditioner outdoor units with trees.

2.2 Grass and moss

Grass or moss type green roof plants can be lifted up over the air-conditioner outdoor units, as shown in Figure 3. Gaps between plant blocks are needed to let cooled air flow through. The hung up plants can shade the solar radiation as well.

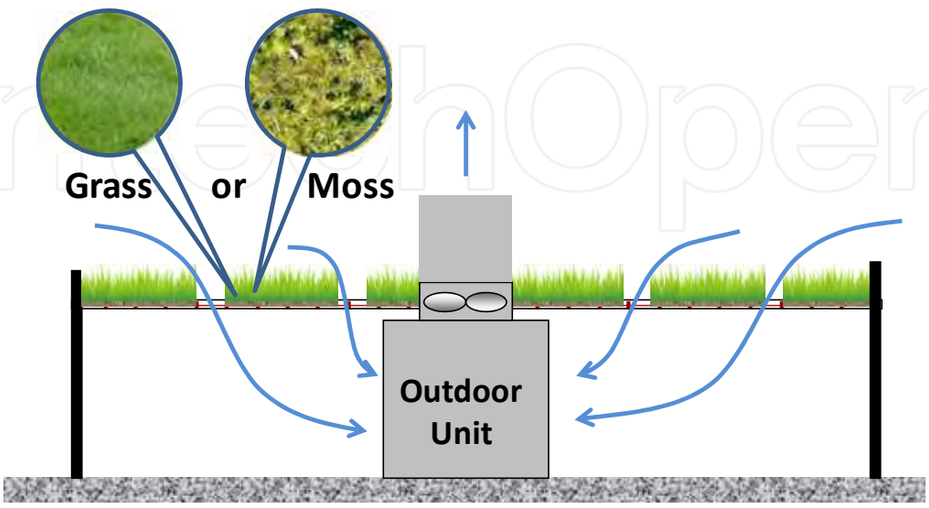

Fig. 3. Combination of air-conditioner outdoor units with hung up grass or moss.

2.3 Vine

Vine type green roof plants are most suitable for combining with air-conditioner outdoor units because of the higher transpiration rate. Further, vine type plants suits for being cultivated using hydroponic technology. Figure 4 shows a typical hydroponic cultivation system, which consists of fertilizer tanks, fertilizing controller, fertilizer adjustment tank, circulation pump, and cultivation unit. Hydroponic technology can use a small area cultivation unit to grow a larger area of plants. So in the area covered by plants, only a small part needs to support the relatively heavy cultivation system, while most part only supports the plant vine, which is so light that its weight can be neglected from the viewpoint of roof supporting ability. Figure 5 shows an example of one hydroponic-cultivated tomato tree. From the figure, it can be seen that the cultivation unit only occupies a small part of the area covered by the plant.

Compared with soil-cultivated green roof, hydroponic-cultivated green roofs are light enough to set on existing buildings, which did not consider the weight of cultivation soil during design phase so it cannot burden the weight. Further, the hydroponic-cultivated green roof plants are light enough to be lifted up over the outdoor unit of air-conditioners, which makes the combination system feasible.

3. Experimental study on the cooling and shading effect of hydroponic-cultivated plant

For the purpose of check the energy saving potential of the combination system, experimental devices are set up on the roof of a five-story office building in Osaka Japan.

The air temperature cooled by the green roof plants, plant transpiration rate, solar radiation shading rate, and inlet and outlet air temperatures at the outdoor unit of an air-conditioner, etc. were measured.

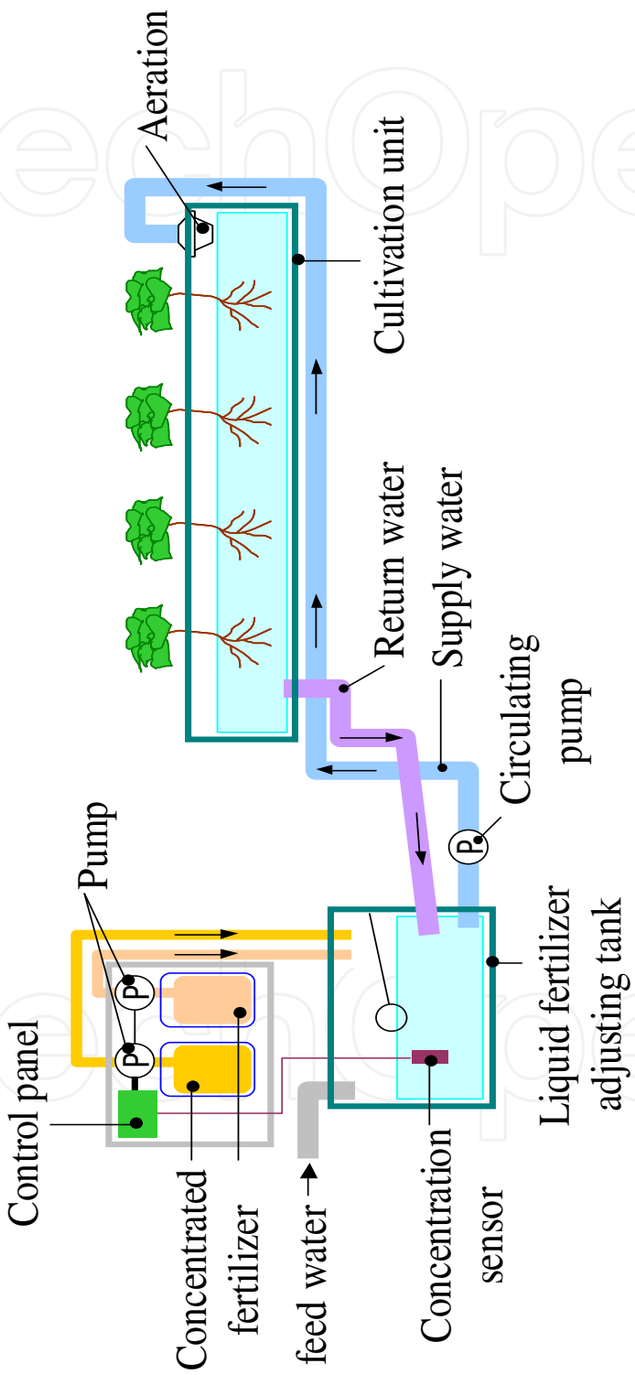

Fig. 4. An example hydroponic cultivation system.

Fig. 5. A hydroponic-cultivated tomato tree (Small floor area occupied by the cultivation-unit compared with the large floor area covered by the plant).

3.1 Experiment setup

Experimental device and measurement points are shown in Figure 6. Measured items and instruments are shown in Table 1. Data are recorded with five minutes interval using a data logger. The hydroponic cultivation device is set on a stage with 1.4 meters height on the roof. The vertical walls of the stage are closed using isolation material to let air can only flow from upside and go through the plants. The upper side of the stage is covered by metal mesh, where the plants spread vines and air can flow through as well. Three ducts equipped with a fan respectively are connected to the south wall of the stage to suck air under the stage, acting as the same function of the outdoor unit fans of air-conditioner.

Sweet potato is selected as the plant because it has high transpiration rate, grows fast, and is strong against wind. The sweet potato was planted on 22nd May 2007. One month later, it began to grow fast with a speed of 0.8 m^2 of horizontal projection area per day until the end of September. Figure 7 shows the plant growing situation at the end of September. In October, its growth slowed down and withered at the beginning of November. So generally speaking, the air-cooling and solar shading effect can be utilized for two months of August and September, which are period with large cooling load. This indicates that the combination system is meaningful for actual application.

For the purpose of check the cooling potential of the plants, the following experiments are conducted.

- Set the flow rate of air flowing through the plants at 2000 m^3/h, 4000 m^3/h, and 6000 m^3/h, to check the relations between temperature decrease and air flow rate.
- Sprinkle water over and under the plants to check how much the air-cooling effect can be improved, focusing on cooling air temperature down as low as to wet-bulb

temperature. Considering it might damage the plants growth, the water sprinkling experiments are conducted twice a day on 11:00 – 12:00 and 14:00 – 15:00.

Mark	Item	Point	Instrument
WD	Wind direction	A	vane-type
WS	Wind speed	A	3-cup anemo meter
RU	Solar radiation	B,D	pyranometer
RD	Solar radiation (under green)	2,3	pyranometer
PAR	Photosynthetically active radiation	D	photon sensor
NRF	Net radiation (roof)	C	net radiometer
NRG	Net radiation (green)	4	net radiometer
IR	Infrared radiation	B	infrared radiometer
WF	Water flow	F	flowmeter
TR	Outside air temperature	A	thermohygrometer
HR	Outside air relative humidity	A	thermohygrometer
TU	Temperature (over green)	1～8	thermocouple thermo recorder
HU	Ralative humidity (over green)	1～8	thermo recorder
TD	Temperature (under green)	1～8	thermocouple thermo recorder
HD	Ralative humidity (under green)	1～8	thermo recorder
TDU	Temperature (in duct)	▲	thermocouple
TL	Leaf temperature	1～4	thermocouple
TW	Wall temperature	×	thermocouple
TF	Floor temperature	⁜	thermocouple
TH	Temperature of suction opening	○	thermocouple
THO	Temperature of supply opening	●	thermocouple

Table 1. Measured items and instruments

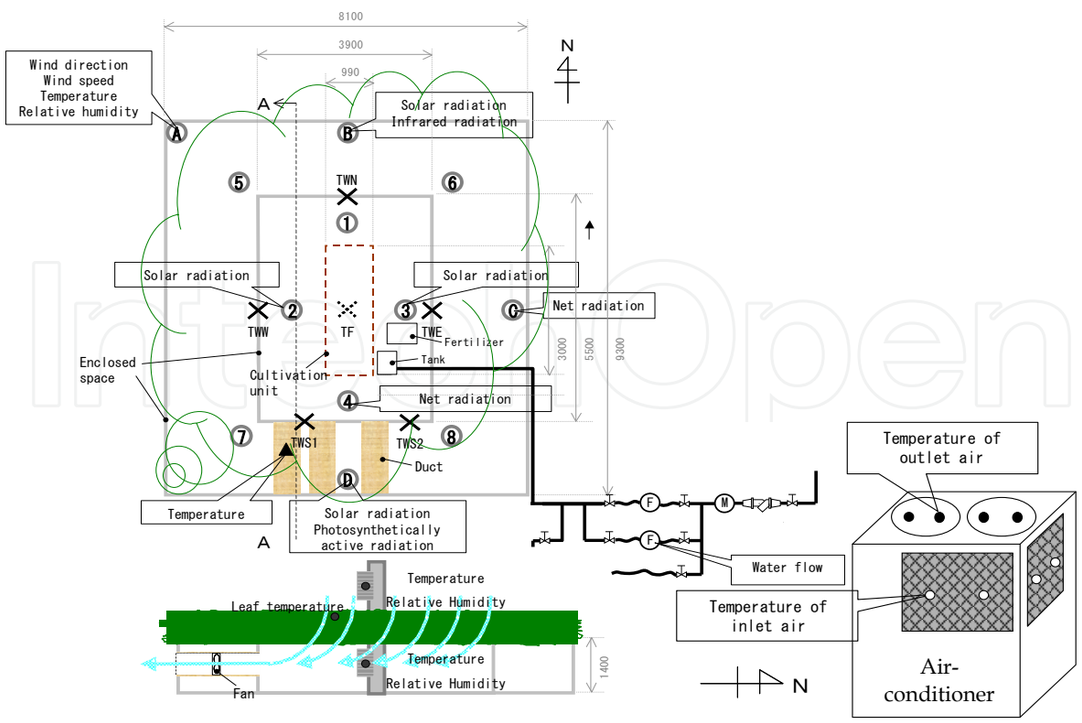

Fig. 6. Experimental device and measurement items.

Fig. 7. Experimental system and plants growing situations at the end of September.

3.2 Experimental results

The experimental period is from August 15th to September 23rd. Although data are recorded 24 hours a day, the cooling affect can only be observed during the period when photosynthetic radiation is active enough to trigger plant transpiration. The observed transpiration and cooling effect are mainly in the period of 10:00 – 16:00, therefore the data during this time are used for analysis.

1) Air temperature decrease

For the experimental period, the daily temperature decreases of maximum, minimum, average of 10:00 – 12:00, and average of 13:00 – 16:00 are as shown in the upper part of Figure 8. The daily average temperature decrease for clear and no-water-sprinkling days is 1.3 ^{o}C. While the average temperature decrease for rainy or water-sprinkle days is 3.0 ^{o}C, which is 2.3 times of that in clear and no-water-sprinkling day. However, the temperature decrease does not differ much for the air flow rate of 2000, 4000, and 6000 m^3/h.

2) Plants transpiration

The daily sum and 10:00 – 16:00 sum of transpired water are shown in the lower part of the Figure 8. The maximum and average daily summed transpirations are 8.3 and 6.3 kg/m^2 horizontal area respectively for clear and no-water-sprinkle days. For the days when water was sprinkled upon the plants, the transpiration is relatively small because leaves were wet and the transpiration temporally stopped.

The comparison of different plant transpiration rate is shown in Figure 9. The maximum daily transpiration rate (kilogram water per square meter of horizontal projection area) of hydroponoic-cultivate sweet potato is 13.8 times of sedum without water-sprinkle and 1.8 times of sedum with water-sprinkle. The maximum transpiration of hydroponoic-cultivate sweet potato is similar to a single tree, which indicates the hydroponoic-cultivate sweet potato can transpire as much water as a tree, while a tree has 20 times more leaf volume per unit horizontal projection area than sweet potato.

3) Solar radiation shading

The solar radiations over and under the plants on a typical day are shown in Figure 10. Even the solar radiation is as high as 1000 w/m², the measured solar radiation under the plants is no more than 10 W/m². That is to say more than 99% solar radiation is shaded by the plants. Therefore hydroponic-cultivated green roof plant can shade solar radiation enough to ignore the influence of solar radiation to the outdoor unit of an air-conditioner.

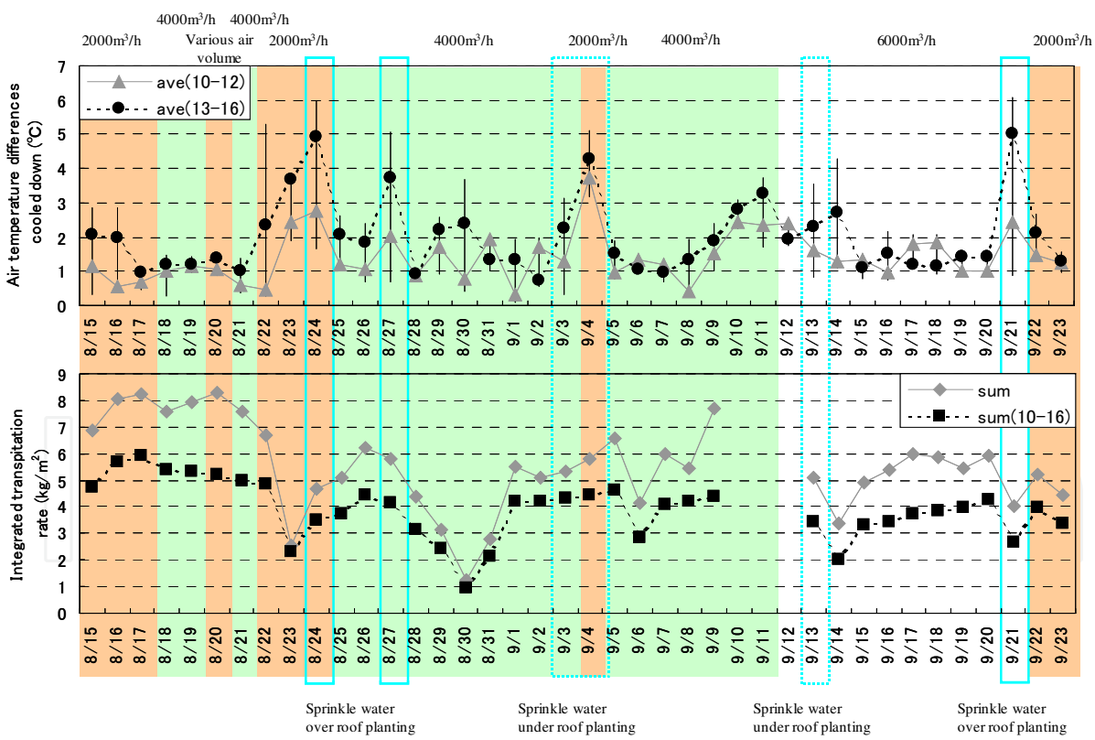

Fig. 8. Experimental results of air temperature decrease (upper graph) and transpiration rate (lower graph).

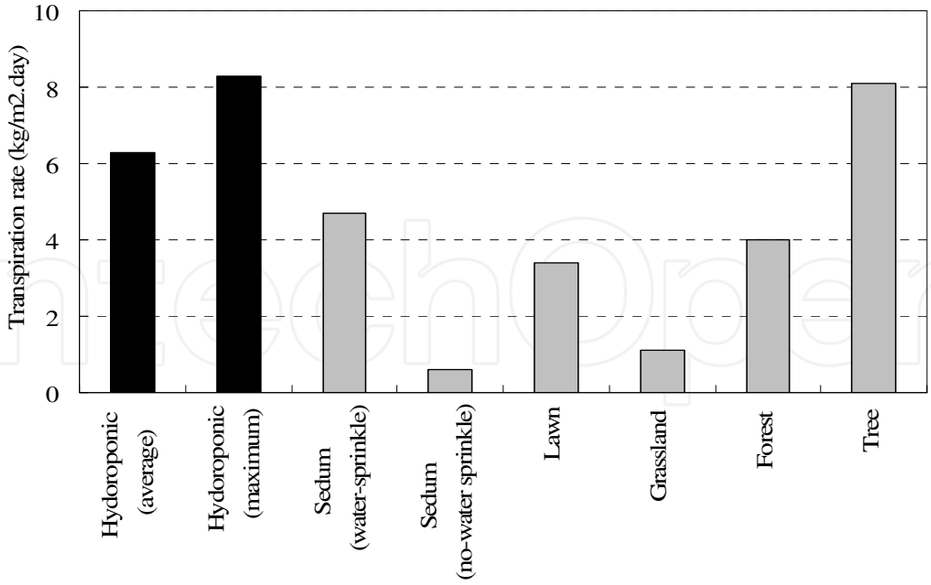

Fig. 9. Transpiration comparison.

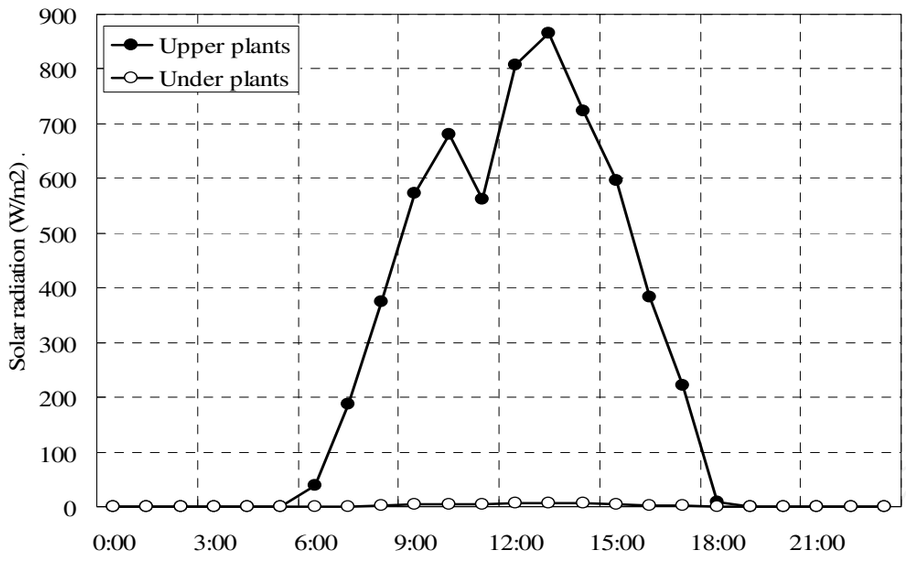

Fig. 10. Solar radiation up and under plants.

4. Estimation of energy saving effect based on experimental data

Based on experimental data, energy saving potential of the combination systems can be estimated using the measured air temperatures before and after being cooled down by the plants and the solar radiation after being shaded.

The calculation flow for estimating the energy saving is shown in Figure 11. Firstly calculate the air cooling effect ΔT caused by plants transpiration and solar shading. Then calculate air-conditioners' energy consumption using an air-conditioner energy consumption model.

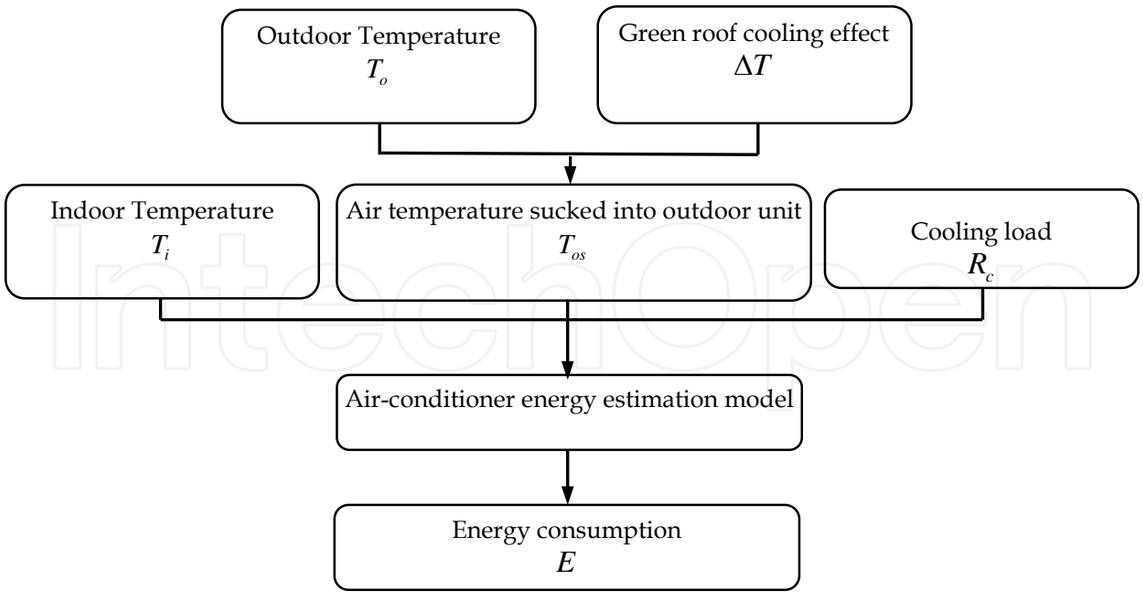

Fig. 11. Calculation flow for energy consumption of air-conditioners.

4.1 Air cooling effect

The air temperature decreasing is caused by two reasons. The first is the plants transpiration. The measured temperature differences between the air over and under the plants are used for the calculation. The second is the equivalent air temperature decrease caused by solar shading. If there is no plant shading, the outdoor unit will absorb solar radiation and its surface temperature will rise. This part of heat will raise the temperature of the air sucked into the outdoor unit. The air-conditioners' energy efficiency will be decreased by the temperature increasing of sucked in air. The air temperature increase is calculated using the following equations.

$$\Delta\theta_s = \frac{q_L + \alpha_S q_S}{mC_{Pa}} \tag{1}$$

4.2 Air-conditioner energy consumption model

A regression model fitted using air-conditioner manufacturer's specification data is used to calculate the air-conditioner's energy consumption (Wang et al., 2005).

$$RE = (a_1{\theta_{of}}^2 + b_1\theta_{of} + c_1)(a_2\theta_i^2 + b_2\theta_i + c_2)(a_3CA^2 + b_3CA + c_3) + d \tag{2}$$

$$\theta_{of} = \theta_o - \Delta\theta_T + \Delta\theta_s \tag{3}$$

The energy saving is calculated for four types of typical air-conditioner made by four different manufactures, including Gas-engine Heat Pump (GHP) and Electricity-driven Heat Pump (EHP). The average nominal primary energy Coefficient of Performance (COP) is 1.4 and manufacture year is 2005. Different manufacturer's air-conditioners have different efficiency improvement ratio accompanying to outdoor temperature decreasing. So the

energy saving is different. The daily average energy savings are shown in Figure 12. The maximum energy saving rate is 12% for the air-conditioners with high efficiency improvement ratio, and 3% for the air-conditioners whose efficiencies improve little accompanying to outdoor air temperature decreasing.

The summed energy savings for the experimental period are shown in Table 2. If water-sprinkle is not conducted, the energy saving ratio is 4% for the air-conditioners with high efficiency improvement ratio, and 1% for the air-conditioners with low efficiency improvement ratio. If water-sprinkle is conducted for two hours a day, the energy saving ratios are 9% and 2% for the air-conditioners with high and low efficiency improvement ratio respectively. Among the total energy saving, about 10% is from solar shading and 90% is from transpiration.

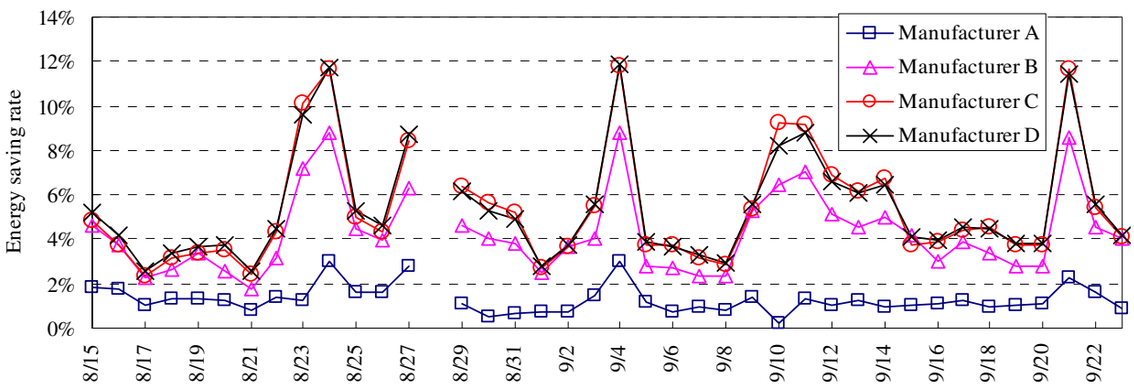

Fig. 12. Estimated daily average energy saving rate achieved by using hydroponic-cultivated sweet potato.

The reasons for why the energy saving ratios at the air-conditioners of the Manufacturer A are roughly 4 times less than these of the others are not further studied because the detailed information is not available about how the air-conditioner operation is tuned corresponding to the different outdoor temperature. The possible reasons might be that different manufactures use different actions or components to tune the running of air-conditioner accompanying to the change of outdoor air temperature. For example if outdoor air temperature decreases, for the air-conditioner with variable speed drive compressor can decrease the compressor's rotational speed to meet the requirement of low compression rate and maintain high efficiency as well. Low compressor rotational speed directly relates to low energy consumption because the energy consumption of air-conditioners is roughly linear to compressor's rotational speed. While for the air-conditioner with constant speed drive compressor can only decrease compression rate through increasing refrigerant flow rate and bypassing the redundant refrigerant flow. The larger flow rate needs larger energy input, which will counteract the energy saving benefitted from the decrease of compression rate. Further the flow rate larger than rated value will cause compressor efficiency decrease. So the energy saving rate might be small when outdoor air temperature decreases.

	Group 1			Group 2			Group 3					
	Manufacturer A (GHP)			Manufacturer B (EHP)			Manufacturer C (GHP)			Manufacturer D (EHP)		
	Energy consumption		Energy saving rate	Energy consumption		Energy saving rate	Energy consumption		Energy saving rate	Energy consumption		Energy saving rate
With or without green roo	With	Without		With	Without		With	Without		With	Without	
sum of Clear and no-water-sprinkle days	2830.5	2859.7	1.0%	2376.4	2449.9	3.0%	2673.1	2767.7	3.4%	2227.6	2317.9	3.9%
sum ofwater-sprinkle days	1024.9	1046.7	2.1%	905.4	970.9	6.7%	965.5	1050.3	8.1%	875.2	963.8	9.2%
sum of rainy days	1011.5	1019.6	0.8%	766.0	810.7	5.5%	857.5	917.6	6.5%	703.4	758.4	7.2%

Table 2. Summed annual energy saving achieved by hydroponic-cultivated sweet potato.

5. Transpiration and cooling effect modeling

Because the energy saving potential estimation results based on experimental result might depend on the local climate conditions, for the purpose of developing a universal method to estimate the energy saving potential, modeling of the transpiration and cooling effect are needed. Therefore it is necessary to develop plant transpiration model, which is used to estimate the plant transpiration rate, and boundary layer model, which is used to calculate the air temperature decreased by plant transpiration.

5.1 Transpiration model

Plants control their transpiration rate by adjusting the opening of stomata, as shown in Figure 13. So the transpiration rate can be calculated through dividing the water vapour partial pressure deficit $(W_i - W_a)$ by the stomatal resistance r_s and boundary layer air resistance r_a, as shown in Equation 4. The resistances can be calculated from their reciprocals, stomatal conductance g_s and boundary layer air conductance g_a, respectively (Equation 5). Boundary layer air conductance g_a is usually used a constant value of 1.13 mol/(m²s) (Kadaira et al., 2005). Here Equation 6 (Campbell and Norman, 1998) is introduced to improve the model accuracy by considering the outdoor wind speed. Regarding the stomatal conductance g_s Jarvis (1976) proposed a model to estimate it using the leave surface temperature T, photosynthetically active radiation (PAR) Q and water vapour saturation pressure deficit D (Equation 7). Based on Jarvis model, Kosugi et al. (1995) improved the models of $f(Q)$, $f(T)$, and $f(D)$ and found that the models shown in Equation 8, 9 and 10 can suit for more plant so these models are used in this research. Further Kadaira et al. (2005) proved through experiment that in Equation 9 ambient air temperature θ can substitute for the leaf surface temperature T with acceptable accuracy. Kadaira et al. (2005) also found that the PAR can be accurately estimated by multiplying global sky radiation J by a correlation coefficient of C_Q with the value of 2.1 (Equation 11). To use these models to estimate the transpiration rate, seven coefficients need to be fitted using the data of the plant that the system uses, i.e. $g_{s\max}$ and a in Equation 5, T_o, T_h, and T_l in Equation 6, b_1 and b_2 in Equation 10.

$$M = \frac{M_w(W_i - W_a)}{r_s + r_a} \tag{4}$$

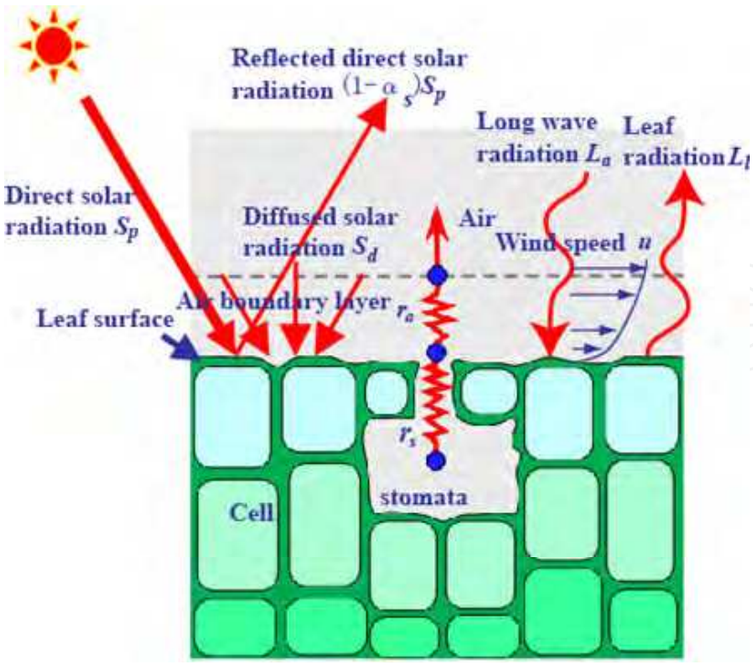

Fig. 13. Plant transpiration mechanisms.

$$r_s = \frac{1}{g_s},\ r_a = \frac{1}{g_a} \tag{5}$$

$$g_a = 0.147 C_t \sqrt{u/l} \tag{6}$$

$$g_s = g_{s\max} \cdot f(Q) \cdot f(T) \cdot f(D) \tag{7}$$

$$f(Q) = \frac{g_{s\max} \cdot Q}{Q + g_{s\max}/a} \tag{8}$$

$$f(T) = \left(\frac{T - T_l}{T_o - T_l}\right)\left\{\left(\frac{T_h - T}{T_h - T_o}\right)^{\left(\frac{T_h - T_o}{T_o - T_l}\right)}\right\} \tag{9}$$

$$f(D) = \frac{1}{1 + (D/n_1)^{n_2}} \tag{10}$$

$$Q = C_Q J \tag{11}$$

The transpiration model is validated using the data measured in the former mentioned experiment.

The measured solar radiation, wind speed, ambient air temperature, plant cooled air temperature, leaf surface temperature, stomatal conductance, transpiration rate, etc. are

used to fit the seven coefficients mentioned above. The fitted coefficients and fitting accuracy (Root Mean Square Error, %RMSE) are shown in Table 3. Then the fitted equations are used to calculate the leaf stomatal conductance and transpiration rate. The calculate transpiration rates are compared with measured ones, as shown in Figure 14. The average and root mean square error (RMSE) are 2.9% and 18.8%, which show that the model accuracy is acceptable for simulation study the energy performance of the combination system.

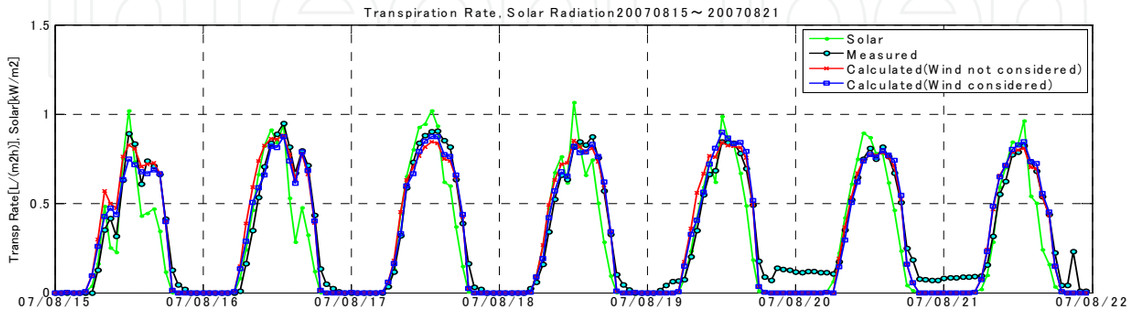

Fig. 14. Comparison of calculated and measured transpiration rate.

$g_{s\max}$	a	b_1	b_2	T_o	T_h	T_l	%RMSE
2.464E+00	5.174E-03	4.898E-01	1.979E+00	3.748E+01	4.350E+01	2.591E+01	8.70%

Table 3. Coefficients fitted for calculating stomatal conductance.

5.2 Boundary layer model

After the transpiration rate is obtained, next step is to use it to calculate how much the air temperature can be decreased by the transpiration. A physical model is considered, as shown in Figure 15.

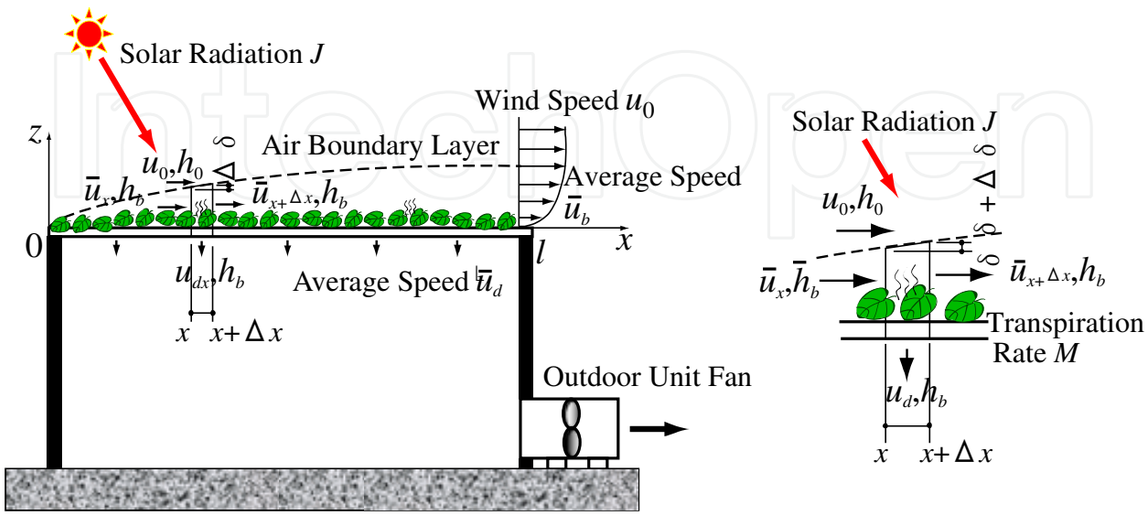

Fig. 15. Air boundary layer model.

When air flows along the plant leaf surface, an air boundary layer forms. If we take a micro air volume with the x-length of Δx, y-length of one meter, and z-length of boundary thickness as the analysis object, the mass conservation is shown in Equation 12 and energy conservation is shown in Equation 13. If the thermal stored in leaf is ignored, the leaf energy conservation is shown in Equation 14. If substituting Equation 14 into Equation 13, the energy conservation will be as shown in Equation 15. Because it is difficult to solve Equation 12 and 15, and what we want to know is not the temperature distribution but the average temperature, we can take the total boundary lay as the analysis object. Thus the mass conservation becomes as shown in Equation 16 and energy conservation becomes as shown in Equation 17. If substituting Equation 14 and Equation 16 into Equation 17, the energy conservation becomes as shown in Equation 18. Further, because the volume of boundary layer V_b is so small (it is 88.7 m^3 for the green roof with a length of 10 m when calculating using boundary layer thickness Equation 20 (Kato, 1964) and boundary layer volume Equation 21) comparing to the air volume entering the boundary layer (usually several thousands m^3/h) that it is safe to ignore the energy change of boundary layer air, i.e. $\Delta H \approx 0$. Therefore energy conservation becomes as shown in Equation 19. The physical meaning of Equation 19 is that the solar radiation energy absorbed by plant leaves becomes the energy difference between the air flowing into and flowing out of the boundary layer if the leaves temperature change and boundary layer air energy change are ignored.

$$u_0\Delta\delta + \overline{u}_x\delta - \overline{u}_{x+\Delta x}(\delta+\Delta\delta) - u_{dx}\Delta x = 0 \tag{12}$$

$$[\rho_0 u_0\Delta\delta h_0 + \rho_b\overline{u}_{b,x}\delta h_x - \rho_b\overline{u}_{b,x+\Delta x}(\delta+\Delta\delta)h_{x+\Delta x} - \rho_b u_{d,x}\Delta x h_x - q\Delta x + M\Delta x r_w]\Delta t = \Delta H \tag{13}$$

$$\alpha J + q - r_w M = 0 \tag{14}$$

$$[u_0\rho_0\Delta\delta h_0 + \rho_b\overline{u}_{b,x}\delta h_x - \rho_b\overline{u}_{b,x+\Delta x}(\delta+\Delta\delta)h_{x+\Delta x} - \rho_b u_{d,x}\Delta x h_x + \alpha J\Delta x]\Delta t = \Delta H \tag{15}$$

$$u_0\delta_l - \overline{u}_b\delta_l - \overline{u}_d l = 0 \tag{16}$$

$$\left(h_0\rho_0 u_0\delta_l - \overline{h}_b\rho_b\left(\overline{u}_b\delta_l + \overline{u}_d l\right) - ql + Mlr_w\right)\Delta t = \Delta H \tag{17}$$

$$\left(h_0\rho_0 u_0\delta_l - \overline{h}_b\rho_b u_0\delta_l + \alpha Jl\right)\Delta t = \Delta H \tag{18}$$

$$h_0\rho_0 u_0\delta_l - \overline{h}_b\rho_b\overline{u}_0\delta_l + \alpha Jl = 0 \tag{19}$$

$$\frac{\delta}{x} = 0.380\Big/\left(\frac{u_0 x}{\nu}\right)^{1/5} \tag{20}$$

$$V_b = \int_0^l \delta dx = 0.211\left(\frac{u_0}{v}\right)^{-1/5} l^{9/5} \tag{21}$$

Further, from Equation 16, we can deduce the speed $\overline{u}_b$ of the air flowing out of boundary layer at the end of the plant stage, as shown in Equation 22. If wind speed u_0 is small, the

$\overline{u}_b$ might be minus. This means the air volume sucked by the air-conditioner fan is large enough to suck all the boundary layer air to the underside of the plant. When $\overline{u}_b$ <0, the energy conservation will become as shown in Equation 23. From Equation 19 and 23, we can deduce the equation for calculating the average enthalpy of boundary layer air $\overline{h}_b$, as shown in Equation 24. Same as the enthalpy, the equations for calculating humidity ratio $\overline{x}_b$ can be deduced, as shown in Equation 25. Where, the average speed of air flowing into the underside of plant is calculated using Equation 26. Further from the enthalpy definition Equation 27, we can deduce the equation for calculating air temperature, as shown in Equation 28. Thus, the air temperature changed by the plant transpiration $\Delta\theta_T$ can be calculated, as shown in Equation 29.

$$\overline{u}_b = u_0 - \overline{u}_d \frac{l}{\delta_l} \tag{22}$$

$$h_0\rho_0 u_d l - \overline{h}_b \rho_b \overline{u}_d l + \alpha J l = 0 \tag{23}$$

$$\begin{aligned} \overline{u}_b > 0 &: \overline{h}_b = \frac{h_0\rho_0 u_0 \delta_l + \alpha J l}{\rho_b u_0 \delta_l} \\ \overline{u}_b < 0 &: \overline{h}_b = \frac{h_0\rho_0 \overline{u}_d + \alpha J}{\rho_b \overline{u}_d} \end{aligned} \tag{24}$$

$$\begin{aligned} u_b > 0 &: \overline{x}_b = \frac{x_0\rho_0 u_0 \delta_l + M l}{\rho_b u_0 \delta_l} \\ u_b < 0 &: \overline{x}_b = \frac{x_0\rho_0 \overline{u}_d + M}{\rho_b \overline{u}_d} \end{aligned} \tag{25}$$

$$\overline{u}_d = \frac{V}{l} \tag{26}$$

$$\overline{h}_b = C_{pa}\overline{\theta}_b + \overline{x}_b\left(C_{pw}\overline{\theta}_b + r_{w0}\right) \tag{27}$$

$$\overline{\theta}_b = \frac{\overline{h}_b - \overline{x}_b r_{w0}}{C_{pa} + \overline{x}_b C_{pw}} \tag{28}$$

$$\Delta\theta_T = \theta_0 - \overline{\theta}_b \tag{29}$$

To check the model accuracy, the measured air temperature changes are compared with the model calculated ones from August 15 to September 23. The comparison of the first one week is shown in Figure 16. The average error of the whole comparison period is 3.32% and the %RMSE is 94.02%. The model accuracy is not so high. But considering that the model is a totally physical model so it can be easily used for all situations, the model is acceptable for the further simulation study.

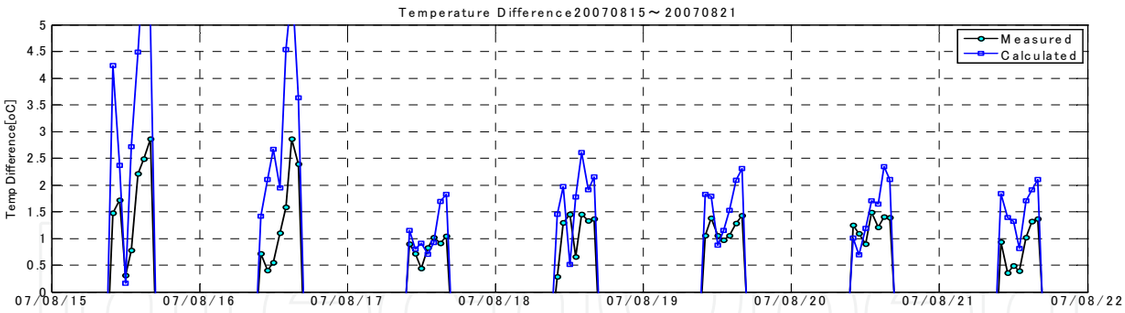

Fig. 16. Comparison of calculated and measured air temperature difference.

6. Methodology for predicting energy saving effect using simulation

6.1 Simulation flow

The flow of predicting the energy saving of the combination system is shown in Figure 17. The following five modules are used to calculate the energy savings.

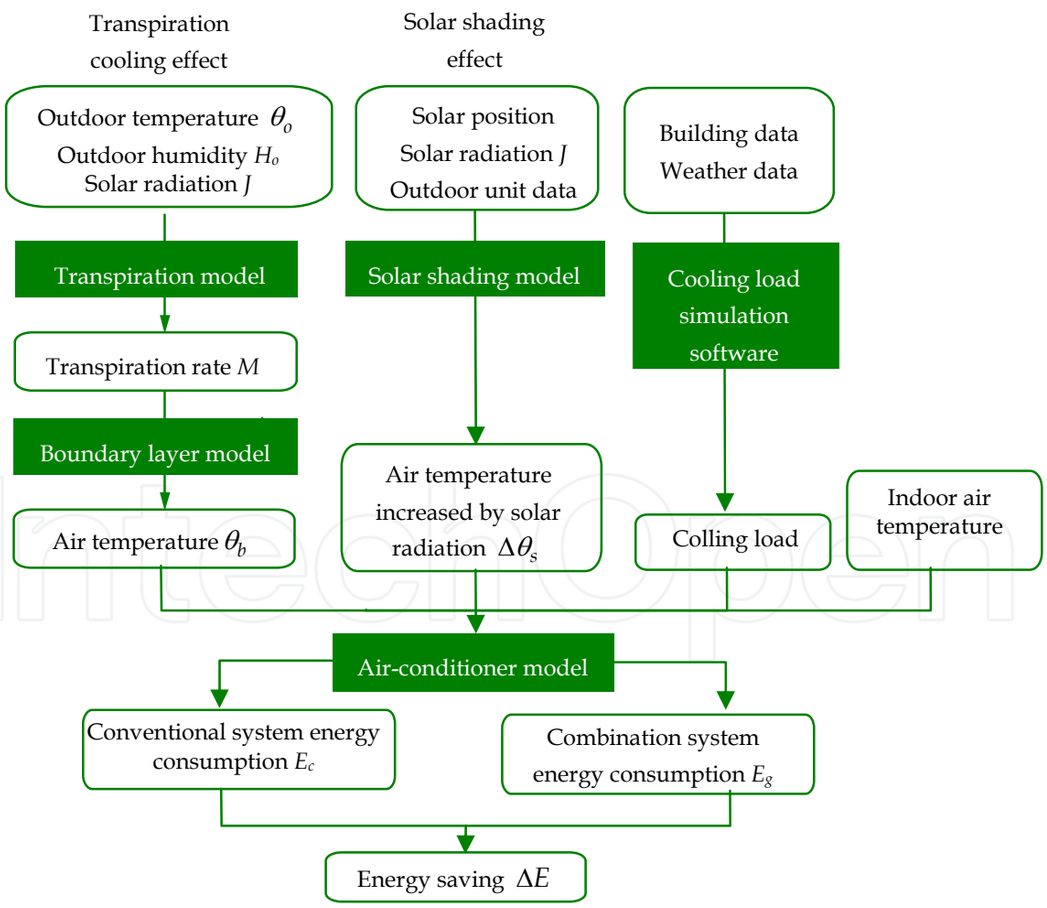

Fig. 17. The flowchart of predicting energy consumption of the system combining the green roof plants with air-conditioner outdoor units.

1. The plant transpiration model, which is used to estimate the plant transpiration rate M.
2. Boundary layer model, which is used to calculate the air temperature θ_b , which is the temperature after being decreased by plant transpiration.
3. Solar shading model (Equation 1), which is used to consider the solar shading effect.
4. Cooling load simulation software, which is used to simulated the cooling load of a given building.
5. Air-conditioner model, which is used to calculate an air-conditioner's energy consumption give the outdoor air temperature, indoor air temperature, and cooling load. The regression model fitted using manufacturers' specification data is used (Equation 2).

6.2 Simulation results

The former explained methodology is used to check the energy saving potential of the air-conditioners made by six main air-conditioner manufactures. They are divided into to three groups: high, middle and low improvement of energy efficiency accompanying to the outdoor air temperature decreasing. The cooling loads of a standard office building at four typical climate areas of Sapporo, Tokyo, Osaka, and Naha in Japan are simulated and used to estimate the energy consumed by the three groups of air-conditioner at the conditions of with and without combining outdoor unit with hydroponic-cultivated sweet potato. The results are shown in Table 4. The energy saving rate is similar at four different areas. It is about 8%, 6% and 1% for the high, middle and low efficiency-improvement group respectively.

Manufactuer	Group 1			Group 2			Group 3					
	A			E			C			D		
Energy related to use or not use roof plant	Energy consumption [kWh]		Energy saving rate	Energy consumption [kWh]		Energy saving rate	Energy consumption [kWh]		Energy saving rate	Energy consumption [kWh]		Energy saving rate
	Use	Not Use		Use	Not Use		Use	Not Use		Use	Not Use	
Sapporo	32396.30	32449.91	0.2%	26876.48	28371.19	5.3%	24250.59	26250.85	7.6%	24733.34	26492.37	6.6%
Tokyo	6353.16	6430.23	1.2%	5396.26	5726.88	5.8%	5252.81	5690.67	7.7%	4970.74	5355.23	7.2%
Osaka	10314.08	10438.78	1.2%	9595.27	10211.44	6.0%	8669.72	9465.12	8.4%	9089.36	9880.86	8.0%
Naha	12675.15	12801.64	1.0%	12050.77	12845.89	6.2%	10430.95	11445.15	8.9%	11388.72	12430.08	8.4%

Table 4. Energy saving potentials of the combination system at four typical climate areas.

7. Summary

This chapter describes how to improve energy efficiency of air-conditioners by combining the air-conditioner outdoor units with green roof plants for the purpose of utilizing the plant transpiration cooling effect and solar shading effect.

Experimental system was set up to measure the actual plant cooling and solar shading effect. The measurement results show that: 1) the air temperature can be cooled down by the hydroponic-cultivated sweet potato by 1.3°C in average for clear day and 3°C in average when water was sprinkled; 2) more than 99% solar radiation can be shaded by the plants.

Based on the experimental results, energy saving potential of the combination system was estimated for typical air-conditioners from different manufacturers. The results show that for clear days, the energy saving ratio is about 4% for air-conditioners with high efficiency

improvement ratio and 1% for air-conditioners with low efficiency improvement ratio. If water-sprinkle is conducted two hours per day, the energy savings are 9% and 2% respectively.

Further, plant transpiration model was described, which is used to calculate the transpiration rate. And boundary layer model was described as well, which is used to calculate the temperature decrease caused by the plant transpiration. The models were validated using the experimental data. The validation results show that: 1) the average and %RMSE of transpiration model are 2.9% and 18.8% respectively. The average error of boundary layer model is 3.32% and the %RMSE is 94.02%. The model accuracies are not very high, which imply that the models need further improvement. Considering that the models are physical model and it can be easily used for all situations, the models are acceptable for simulation study.

Finally the methodology of predicting the energy saving potential using the models is explained. Four typical climate areas in Japan are selected to simulate the cooling loads and energy saving potentials of combining green roof plant with air-conditioner outdoor units. The simulation results show that the energy saving rates are similar for the four typical climate regions, which are about 8%, 6% and 1% respectively for the air-conditioners with high, middle and low efficiency-improvement ratio accompanying to air temperature decreasing.

8. Acknowledgement

The research described in this chapter is financially supported by Nissan Science Foundation, the Japan Society for the Promotion of Science (Project No. 17760468, 2004) and the Kansai Electric Power Co. Inc. The hydroponic cultivation system are provided and technically supported by Kyowa Corporation Ltd. Here the grateful acknowledgements are expressed to all the supporters.

9. Nomenclature

a : Reaction efficiency of stoma opening corresponding to light
a_i, b_i, c_i, d, i=1,2,3: Coefficients fitted using manufacturer specification data
CA: Cooling amount produced by an air-conditioner (kW)
C_{pa}: Specific heat of dry air, 1.005 kJ/(kgDA°C)
C_{pw}: Specific heat of water vapor, 1.846 kJ/(kg°C)
C_t: Outdoor wind turbulent coefficient, 1.4
C_Q: Correlation coefficient between PAR and sky global radiation, 2.1
g_a : Conductance of leaf surface boundary layer, mol/m²s
$g_{s\max}$: The maximum stomatal conductance, mol/m²s
g_s : Stomatal conductance, mol/m²s
D : Saturation pressure deficit, kPa
E: Power consumption of air-conditioner, kW
h: Air enthalpy, kJ/kgDA
J: Global sky radiation, kW/m²
l: Length of green roof, m

m : Outdoor unit fan air mass flow rate (kg/s)
M: Transpiration rate, kg/m²s
M_w : Molar mass of water, 0.01802 kg/mol
n_1 : The saturation pressure deficit when stomatal conductance becomes half
n_2 : Curvature of the saturation pressure deficit function
q: Sensible heat exchange between leaves and air, kW/m²
q_L : Long wave radiation between outdoor unit and its surroundings (W)
q_s : Short wave radiation (i.e. global solar radiation) (W)
Q : photosynthetically active radiation (PAR), μ mol/m²s
r_a : Boundary layer resistance, m²s/mol
r_s : Stomatal resistance, m²s/mol
r_{w0} : Latent heat of water evaporation at 0°C, 2501 kJ/kg
T : Leaf surface temperature, °C
T_o : The most proper temperature, °C
T_h : Upper applicable temperature, °C
T_l : Lower applicable temperature, °C
u: Air flow speed, m/s
V: Air volume flow rate, m³/s
W_i : Saturation partial pressure of water vapor at leaf surface, mb/mb
W_a : Water vapor partial pressure, mb/mb
x : Air humidity ratio, kg/kgDA
α : Absorption ratio to short wave radiation, leaves of sweet potato: 0.56; outdoor unit of air-conditioner: 0.76
α_s : Short wave radiation absorption ratio of outdoor unit surface
ρ : Air density, kg/m³
δ : Thickness of boundary layer, m
Δt : Time interval, s
ΔH : Energy change of the air in the boundary layer, kJ
ν : Kinematic viscosity, m²/s
θ : Air dry bulb temperature, °C
θ_i : Indoor air wet bulb temperature, °C
θ_o : Outdoor air dry bulb temperature, °C
θ_{of} : Final outdoor air dry bulb temperature after transpiration cooling and solar radiation absorption, °C
$\Delta\theta$: Change of air dry bulb temperature, °C

Subscription

o: Air out of the boundary layer
b: Air in the boundary layer
d: Air flowing into the underside of green roof plant
g: Use hydroponic-caltivated green roof plant

l: Length of the green roof
L: Long wave
S: Solar radiation
T: Transpiration

Superscript

t : Time step t
$\bar{}$: Average

10. References

Alexandria Eleftheria, Jones Phil (2008), Temperature decreases in an urban canyon due to green walls and green roofs in diverse climates, Building and Environment, Vol. 43, pp. 480–493

Clerk Corrie, Adriaens Peter, Nriantalbot Albot, Talbot F. Brian (2008), Green Roof Valuation: A Probabilistic Economic Analysis of Environmental Benefits, Environmental Science Technology, Vol. 42, pp. 2155–2161

Campbell, G. S. & Norman, J. M. (1998) An Introduction to Environmental Biophysics Second edition. p101, p108, Springer, New York, US

Di H. F. and Wang D. N. (1999), Cooling Effect of Ivy on a Wall, Experimental Heat Transfer, Vol. 12, pp.235-245

Elena Palomo Del Barrio (1998), Analysis of the green roofs cooling potential in buildings, Energy and Buildings, Vol. 27, pp.179-193

Jarvis, P.G. (1976) The interpretation of the variations in leaf water potential and stomatal conductance found in canopies in the field. Phil.Trans.R.Soc.Lond.B, 273, pp.593-610.

Kadaira, A., Yoshida, H., Ito, M. et al. (2005) A study on the climatic mitigation effect of trees in an area around a residential complex. Journal of Environmental Engineering, Architecture Institute of Japan, No. 598, pp. 71-77.

Kato, K. (1964), Heat transfer. Yokendo Co., ltd., p105.

Kumar Rakesh, Kaushik S.C. (2005), Performance evaluation of green roof and shading for thermal protection of buildings Building and Environment, Vol. 40, pp. 1505–1511

Spala A., Bagiorgas H.S., Assimakopoulos M.N., Kalavrouziotis J., Matthopoulos D., Mihalakakou G. (2008), On the green roof system. Selection, state of the art and energy potential investigation of a system installed in an office building in Athens, Greece, Renewable Energy, Vol. 33, pp.173-177

Takebayashi Hideki, Moriyama Masakazu (2007), Surface heat budget on green roof and high reflection roof for mitigation of urban heat island, Building and Environment, Vol. 42, PP. 2971–2979

Wong Nyuk Hien, Chen Yu, Ong Chui Leng, Sia Angelia (2003) Investigation of thermal benefits of rooftop garden in the tropical environment, Building and Environment, Vol. 38, pp.261-270

Wang Fulin, Yoshida Harunori, Masuhara Satoshi, Kitagawa Hiroaki, and Goto Kyoko (2005), Simulation-Based Automated Commissioning Method for Air-Conditioning Systems and Its Application Case Study, Proceedings of the 9th International Building Performance Simulation Association Conference, Montreal, Canada, pp. 1307-1314

Wang Fulin, Yoshida Harunori, Yamashita Michiko, Improving Air-conditioners' Energy Efficiency Using Hydroponic Roof Plants, Proceedings of the 29th AIVC Conference in 2008, pp. 131-136, 2008.10

Wang Fulin, Yoshida Harunori, Yamashita Michiko, Prediction of the Energy Savings of a System Combining Air-conditioner's Outdoor Unit with Hydroponic-cultivated Roof Plant, Proceedings of the 6th International Symposium on Heating, Ventilating and Air Conditioning - ISHVAC09, Nanjing, China, pp. 419-427, 2009.11

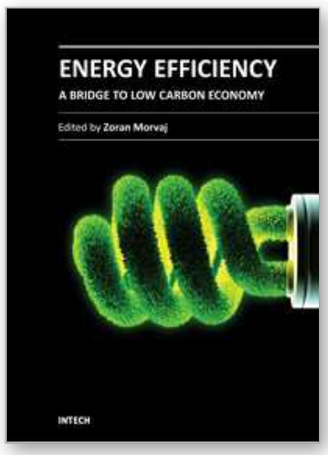

Energy Efficiency - A Bridge to Low Carbon Economy
Edited by Dr. Zoran Morvaj

ISBN 978-953-51-0340-0
Hard cover, 344 pages
Publisher InTech
Published online 16, March, 2012
Published in print edition March, 2012

Energy efficiency is finally a common sense term. Nowadays almost everyone knows that using energy more efficiently saves money, reduces the emissions of greenhouse gasses and lowers dependence on imported fossil fuels. We are living in a fossil age at the peak of its strength. Competition for securing resources for fuelling economic development is increasing, price of fuels will increase while availability of would gradually decline. Small nations will be first to suffer if caught unprepared in the midst of the struggle for resources among the large players. Here it is where energy efficiency has a potential to lead toward the natural next step - transition away from imported fossil fuels! Someone said that the only thing more harmful then fossil fuel is fossilized thinking. It is our sincere hope that some of chapters in this book will influence you to take a fresh look at the transition to low carbon economy and the role that energy efficiency can play in that process.

How to reference
In order to correctly reference this scholarly work, feel free to copy and paste the following:

Fulin Wang and Harunori Yoshida (2012). Improving Air-Conditioners' Energy Efficiency Using Green Roof Plants, Energy Efficiency - A Bridge to Low Carbon Economy, Dr. Zoran Morvaj (Ed.), ISBN: 978-953-51-0340-0, InTech, Available from: http://www.intechopen.com/books/energy-efficiency-a-bridge-to-low-carbon-economy/improve-energy-efficiency-of-air-conditioner-using-green-roof

INTECH
open science | open minds

InTech Europe
University Campus STeP Ri
Slavka Krautzeka 83/A
51000 Rijeka, Croatia
Phone: +385 (51) 770 447
Fax: +385 (51) 686 166
www.intechopen.com

InTech China
Unit 405, Office Block, Hotel Equatorial Shanghai
No.65, Yan An Road (West), Shanghai, 200040, China
中国上海市延安西路65号上海国际贵都大饭店办公楼405单元
Phone: +86-21-62489820
Fax: +86-21-62489821

IntechOpen